Radiation ionization energy in *a*-Si:H

J. Dubeau,* L. A. Hamel,† and T. Pochet‡
Groupe de Recherche en Physique et Technologie des Couches Minces (GCM), Département de Physique, Université de Montréal, P.O. Box 6128, Downtown Station, Montréal, Québec, Canada H3C 3J7
(Received 10 August 1995; revised manuscript received 16 January 1996)

The radiation ionization energy ε_p, which is the mean energy expended per electron-hole pair generated in a given material by an ionizing radiation, is one of the most important parameters governing the properties of radiation detectors based on this material. Since the advent of semiconductor detectors in the 1950s, a great deal of experimental and theoretical work has been done to determine values of ε_p for various crystalline semiconductors. After some review of the theoretical models proposed for crystalline semiconductors, we present a detailed study for an amorphous semiconductor. A microscopic Monte Carlo calculation, taking into account the actual density of states, was performed in *a*-Si:H to study the energy sharing between ionization and phonon production during hot carrier thermalization. This simulation yields values from 4.3 to 5.0 eV for ε_p for reasonable values of the phonon emission mean free path λ_r in *a*-Si:H. This result is in agreement with experimental results of about 4.4 eV and are comparable to 3.63 eV in crystalline silicon, despite the larger 1.7-eV gap.

I. INTRODUCTION

When an energetic ionizing particle enters a condensed material, it gradually transfers its energy to the material through numerous interaction events, among which are electron excitation, ionization, nuclear displacement, and lattice excitation. At each ionization event, energetic secondary carriers are produced, which, in turn, are subjected to the same processes. A cascade is thus generated in which the number of free carriers increases as their energy decreases. The carrier multiplication stops when none of these have enough energy to produce further impact ionization. The details of this cascade are very complex because it involves a large number of particles and many different physical processes on a wide energy range. Due to its stochastic nature, each cascade is unique and one is usually mostly concerned with the average final state, i.e., how the initial energy has been shared between various physical processes. A detailed analytic description is very difficult in real cases and Monte Carlo simulations are best suited to such questions.

The electric signal produced by a semiconductor particle detector is directly related to these processes. Indeed, in a usual diode detector, if no charge loss occurs due to trapping or recombination, the collected charge is equal to the number of electron-hole pairs produced in the cascade. The charge output from such a detector has been observed to be directly proportional, to a high degree of accuracy, to the energy deposited in the detector by the incident particle. The ratio of the deposited energy to the number of generated pairs is then ε_p, the mean energy expended per electron-hole $(e\text{-}h)$ pair, and is called the radiation ionization energy. Furthermore, ε_p has been observed to be fairly independent of the particle species, being a characteristic of the material only.

Several measurements of ε_p have been reported for various crystalline semiconductors (such as Si, Ge, GaAs, GaP, InP, CdS, SiC, InSb, and HgI_2) at different temperatures. These indicate that ε_p is about three to four times larger than the bandgap E_g. The difference between ε_p and E_g is the average energy lost to nonionizing processes. The observation that ε_p is mostly independent of the incident particle energy from a few times E_g up to many GeV indicates that its value is totally determined by low-energy processes occurring at the very end of the cascade. In fact, only impact ionization and phonon production, from a few eV above the band edge, have to be considered; all nonionizing processes other than phonon generation playing a negligible role. Some models have been proposed to explain the roughly linear relationship between ε_p and E_g in crystalline semiconductors. In a few cases, explicit calculations have been made, taking into account the detailed electronic structure of a given material, to obtain ε_p. Some of these models are described in Sec. II in order to identify the approach that seems best suited for the case of hydrogenated amorphous silicon (*a*-Si:H).

Our Monte Carlo simulations are described in detail in Sec. III. The physical assumptions are discussed first. Then the electronic density of states (EDOS) used in the calculations is presented. The expressions for the ionization and phonon production rates are given and the relative normalization between these rates is discussed. Finally, the simulation algorithm is presented. The results of the simulations, both for crystalline silicon (*c*-Si) and hydrogenated amorphous silicon (*a*-Si:H), are given in Sec. IV. A discussion follows in Sec. V and conclusions are stated in Sec. VI.

II. PREVIOUS MODELS USED FOR CRYSTALLINE SEMICONDUCTORS

In this section, we review some theoretical models proposed to explain the observed values of ε_p in various crystalline semiconductors. The main experimental facts that had to be accounted for were the almost complete independence of ε_p on the deposited energy and the more or less linear relationship between E_g and ε_p. This observed linearity seemed to be valid for all semiconductors as well as for a given semiconductor when the change in E_g was due to a

change in temperature.[1] The independence of ε_p on the incident particle energy down to a few eV indicates that only the interactions of hot carriers near the band edges must be considered in order to understand the energy sharing between ionization and phonon scattering. These models fall into three main categories: some involve the calculation of the various terms of an energy balance equation while others attempt a direct calculation of the mean number of pairs produced by a carrier of a given initial energy. Finally, some models[2,3] consider plasmons as an intermediate step such that ε_p depends on $\hbar\omega_{\rm pl}$, the plasmon energy; these are especially useful to account for the relatively low values of ε_p in insulators. But since we are only concerned here with c-Si and a-Si:H, for which materials the plasmon energy is sufficiently larger than the gap, plasmons are not expected to affect the value of ε_p and these models will not be considered further.

A. Models based on the energy balance equation

Energy conservation allows us to write $\varepsilon_p = E_g + \langle E_L \rangle$, where $\langle E_L \rangle$ is the mean energy loss to nonionizing processes for each pair produced. From measurements in c-Si, McKay[4] found $\langle E_L \rangle_{c\text{-Si}} \sim 2.5$ eV. The first detailed description of hot carrier thermalization was given by Shockley.[5] Only two processes were considered: ionization, characterized by a mean free path λ_i, and Raman phonon emission with a mean free path λ_r. According to Shockley, a hot carrier thermalizes through these processes until it reaches below the impact ionization threshold energy E_i, where ionization is no longer possible. When all carriers are below E_i, their populations are characterized by the average residual energies $\langle E_K \rangle_e$ and $\langle E_K \rangle_h$ for electrons and holes, respectively. Shockley writes the balance equation,

$$\varepsilon_p = E_g + \langle E_K \rangle_e + \langle E_K \rangle_h + r\hbar\omega_r , \tag{1}$$

where $r = \lambda_i/\lambda_r$ is the mean number of Raman phonons produced between two successive ionization events and is taken to be energy independent. Assuming parabolic bands, equal threshold energies for electrons and holes, and uniform final populations in the Brillouin zone, Shockley finds $\langle E_K \rangle_e = \langle E_K \rangle_h = \frac{3}{5} E_i$. Using the parameters $E_i = E_g$, $r = 17.5$, and $\hbar\omega_r = 63$ meV, Eq. (1) yields $\varepsilon_p = 3.5$ eV for c-Si.

Other models differ from the previous one only in the values of the parameters. For example, Klein[6] uses $E_i = \frac{3}{2} E_g$ as suggested by the latest avalanche data and as expected from energy and momentum conservation in the simplest case of a direct gap, parabolic bands with equal effective masses for electrons and holes, and uniform final carrier distributions in **k** space. Klein obtains the result

$$\varepsilon_p = \tfrac{14}{5} E_g + r\hbar\omega_r . \tag{2}$$

Klein noted that $r = \lambda_i/\lambda_r$ must be energy dependent and that $r\hbar\omega_r$ actually represents a weighted average over the carrier energy distributions. He further observed that this term seemed fairly independent of the material and that his expression, with $0.5\ \text{eV} < r\hbar\omega_r < 1$ eV, reasonably reproduced all known values of ε_p when E_g stands for the smallest gap, whether direct or indirect. But when more precise experimental values of ε_p or new materials are considered, this universality of Klein's formula is less convincing.[7] In particular, for SiO_2 with a gap of 8.5 eV, $\varepsilon_p = 18$ eV, much less than 25 eV as given by the model. In the case of a-Si:H whose optical gap is 1.7 eV, Klein's model predicts $\varepsilon_p = 5.8$ eV while our experimental measurement indicates a value between 3.4 and 4.4 eV,[8–11] much closer to the c-Si value than to the model's prediction. It is mainly to understand this low value of ε_p in a-Si:H as compared with crystalline semiconductors of similar E_g that the present work was undertaken.

B. Models based on calculating the interaction rates

Other models involve an analytical calculation or numerical simulation of the cascade. This requires explicit expressions for the two scattering processes that are of importance in hot carrier thermalization, namely, ionization and optical-phonon scattering.

The ionization rate $W_{i(e,h)}(E)$, for electrons or holes in c-Si, was calculated by Kane,[12] using first-order time-dependent perturbation theory. All allowed transitions, i.e., E and **k** conserving, that promote an electron from the valence to the conduction band are summed. The transition matrix element M_{if}, the expectation value of the Coulomb interaction, is calculated, using the actual silicon band structure. However, Kane observed that the result is unchanged if M_{if} is assumed constant and **k** conservation is ignored. In other terms, all energy conserving transitions are equally probable and the ionization rate is obtained from summing over all available states. For electrons,

$$W_{ie}(E) = A_{ie} \int_{E_F}^{E} dE_1\ g(E_1) \int_{-E}^{E_F} d\varepsilon\ g(\varepsilon) g(E - |\varepsilon| - E_1), \tag{3}$$

where g denotes the EDOS, E is the incident energy of the initial electron, ε is the energy of the resulting hole, E_1 is the energy of the resulting electron, and A_{ie} is a constant factor. Such a simple expression has been used in many instances to analyze photoemission data in c-Si as well as in other materials.[13] A similar expression is found for $W_{ih}(\varepsilon)$, and Kane found that numerical values of $W_{ie}(E)$ and $W_{ih}(\varepsilon)$ were virtually identical for energies E and ε at equal distance from the band edges.

In c-Si, a number of experimental observations, such as the temperature dependence of the phonon limited mobility μ_{ph} (Ref. 14) and the saturation velocity at high electric field,[15] are explained by invoking hot electron interaction with energetic phonons only. Moreover, at room temperature, phonon absorption may be neglected. Considering only Raman phonon ($\hbar\omega_r$) emission, the scattering rate is

$$W_{re}(E) = A_{re} g(E - \hbar\omega_r). \tag{4}$$

1. Drummond and Moll's model

Drummond and Moll[16] numerically calculated the various terms of Shockley's energy balance equation for the case of c-Si. To do so, they wrote recursion relations for the probability $P_m(E)$ that an electron of initial energy E produce an electron-hole pair after exactly m phonon scattering events,

$$P_0(E) = \frac{W_i(E)}{W_i(E) + W_r(E)}, \tag{5}$$

$$P_m(E)=(1-P_0)\cdots(1-P_{m-1}) \times\frac{W_i(E-m\hbar\omega_r)}{W_i(E-m\hbar\omega_r)+W_r(E-m\hbar\omega_r)}, \quad (6)$$

which involve the energy dependent rates of ionization $W_i(E)$ and of phonon scattering $W_r(E)$. Similar expressions are found for hot holes. The average energy loss to phonons between two ionization events $\langle E_r\rangle_{(e,h)}$ is given by the expectation value of m, i.e., $\langle E_r\rangle_{(e,h)}=\langle m\rangle_{(e,h)}\hbar\omega_r$. The energy distributions of carriers that are no longer capable of ionization are then computed by a Monte Carlo simulation. Their mean values yield $\langle E_K\rangle_{(e,h)}$. These distributions are found to be nonuniform in the Brillouin zone, thus indicating that previous models were oversimplified. The authors used the following simple expressions for the interaction rates:

$$W_{i(e,h)}(E)=A_{i(e,h)}|E-E_g|^{4.2}, \quad |E|>E_g \quad (7)$$

$$W_{r(e,h)}(E)=\text{const}, \quad |E|>E_g, \quad (8)$$

where the electron or hole energy E is measured from the band edge. $W_{i(e,h)}(E)$ closely fits the rates that had been calculated by Kane[13] and the approximation of a constant value for $W_{r(e,h)}(E)$ is justified at least for energies more than 2 eV from the band edge. Of particular importance is the relative normalization of these rates. From photoemission data,[17] Drummond and Moll find a normalization $r(E)=W_{re}(E)/W_{ie}(E)=2.18$ at 5 eV above the conduction-band edge. This yields $\varepsilon_p=4.24$ eV for c-Si. Noting that the calculated rates and the normalization may not be accurate, they indicate that a normalization $r(E)=0.6$ at 5 eV above E_C (where C is conduction band) would be needed to yield $\varepsilon_{p_{c\text{-Si}}}=3.6$ eV.

2. Calculation of the mean number of pairs produced

Instead of expressing the ionization energy ε_p as a sum of terms in an energy balance equation, another approach is to calculate directly, from the ionization and scattering rates, the average number of pairs $n_p(E)$ produced by an initial carrier of energy E. The ionization energy is then obtained from its definition,

$$\varepsilon_p=\frac{E}{n_p(E)}. \quad (9)$$

Since the interaction rates W_i and W_r are constrained by the requirement of energy conservation, both methods should yield similar results. Antončik, Di Cola, and Farese[18] showed that these rates obey integro-differential equations. But solving these equations to extract $n_p(E)$ requires explicit expressions for the rates over a broad energy range and results were given only for a few extremely simplified band models. Results indicate that n_p rises steeply from 0 to 1 slightly above E_i and increases almost linearly above $\sim 3E_g$. This shows striking resemblance with quantum yield measurements in Ge (Ref. 19) and Si (Ref. 20). In both cases, the slope of $\eta(E)$ above a few eV is found to provide the same value of ε_p as that obtained with high-energy particles, thus indicating that ε_p is determined only by low-energy processes.

Using a slightly different approach, Alig, Bloom, and Struck[8] found recursion relations for $p_n(E)$, the probability that a carrier of energy E produce n pairs. The mean number of pairs $\langle n_p(E)\rangle$ is then simply $\Sigma n p_n(E)$, the expectation value of n, and is observed to depend only slightly on the threshold energy E_i with interaction rates calculated for parabolic and isotropic bands. In c-Si, using the normalization $W_r/W_i=1.6$ at 5 eV above E_C, compatible with measurements from Bartelink, Moll, and Meyer,[17] they find $\varepsilon_p=3.6$ eV.

C. Conclusions

The various models by Shockley, Klein, and others, based on the energy balance, appear to provide only approximate results for ε_p and it is not surprising that they may fail for new materials and especially for amorphous semiconductors as a-Si:H. First, the hypothesis of uniform distributions of residual kinetic energies in the Brillouin zone, for crystalline materials, is contradicted by calculations by Drummond and Moll. Second, ionization threshold energies cannot be defined in amorphous semiconductors. Finally, the constant value of the $r\hbar\omega_r$ term in Klein's formula [Eq. (2)] that is used to predict ε_p for a given material has no physical basis. The discrepancy between our experimental value of ε_p between 3.4 and 4.4 eV (Refs. 8–11) and the value of 5.8 eV from Klein's formula in a-Si:H is then less surprising. To understand the low value of ε_p in a-Si:H, we must proceed with a detailed Monte Carlo simulation of hot carrier thermalization, using realistic descriptions of the ionization and phonon-scattering rates.

III. MONTE CARLO

Our calculation of ε_p follows the same lines that were introduced by Drummond and Moll and in which many cascades produced by initial carriers with a given energy distribution are generated by a Monte Carlo simulation. ε_p is obtained from the slope of the average number of pairs produced as a function of the initial energy. We first describe the principles of the simulation. The electronic density of states used to calculate the ionization rate is then presented. Next, the interaction rates and their relative normalization are discussed. Finally the Monte Carlo algorithm is described. The results of the simulations are presented in Sec. IV.

A. General principles of the simulation

1. Initial carrier distributions

Before a cascade may be generated, the initial distributions of energetic carriers, $S_e(E)$ and $S_h(\varepsilon)$, must be given. Two types of distributions have been considered. First, a δ-type distribution is used, in which carriers of one type only (electrons or holes) are injected at a constant initial energy. When many cascades have been simulated for a given initial energy E, the energy is increased and new events are generated. The number of generated pairs is then found to increase linearly with E above a few eV and ε_p is given by

$$\frac{1}{\varepsilon_p}=\frac{\partial n_p}{\partial E}. \quad (10)$$

Second, in order to study the yield for UV light, initial distributions due to the absorption of photons of energy E_γ are

calculated. The initial number of electrons and holes are then equal, $N_e=N_h=N_\gamma$, and their distributions are determined by the requirement of energy conservation ($E_\gamma=E+|\varepsilon|$) and the absorption probability by an electron at energy ε in the valence band,

$$\alpha(\varepsilon,E_\gamma)\propto g(\varepsilon)f(\varepsilon)g(\varepsilon+E_\gamma)[1-f(\varepsilon+E_\gamma)]. \quad (11)$$

Many events are thus generated for initial distributions corresponding to several photon energies. The function $n_p(E_\gamma)$ is again linear above a few eV and ε_p is obtained from

$$\frac{1}{\varepsilon_p}=\frac{\partial n_p}{\partial(E_\gamma)}. \quad (12)$$

In previous studies of signal generation in crystalline semiconductors, electron and hole energies were usually referred from their respective band edge. For *a*-Si:H where there is a continuum of states extending into the mobility gap, both E and ε are measured from the Fermi level E_F; electrons are given positive energies while holes have negative energies.

2. Cascade generation

Hot carriers undergo a sequence of ionization and scattering events that is determined by the interaction probabilities. For an electron of energy E, the probability $P_{0e}(E)$ that the next event be ionization is given by Eq. (5) and the probability that the next event be phonon emission is

$$P_{re}(E)=1-P_{0e}(E). \quad (13)$$

When phonon emission occurs, the carrier energy is reduced to $E-\hbar\omega_r$. In the case of ionization, the final state consists of two electrons and one hole of energies E_1, E_2, and ε, respectively.

The carrier populations will thus increase until ionization is no longer possible. For ideal crystalline materials with a gap of zero state density, there is a well-defined ionization threshold but for amorphous semiconductors where there is a non-negligible density of localized states in the mobility gap, ionization due to a transition between extended and localized states is possible. This means that, allowing sufficient time, all carriers will fall into the localized states. Since we want to determine the number of free carriers initially produced by an incident radiation prior to charge collection, we must here distinguish between prompt processes, which are fast compared to charge collection, from other processes occurring on longer time scales. Among these, the ''slow'' thermalization of carriers, a few kT above the band edge, and thermal detrapping are the basic processes leading to multitrapping dispersive transport.[21] A line is then drawn, somewhat arbitrarily, between these two regimes by considering in our simulation that transitions from extended to localized states due to phonon emission and transitions between two localized states are forbidden. The cascade will then stop when all carriers are at or below the band edge and the simulation will provide the average number of carriers and their distributions at the end of the ''prompt'' processes.

B. Electronic density of states in *a*-Si:H

An accurate description of the EDOS of a material is essential for a realistic calculation of the scattering rates. Since various parts of the EDOS are probed by rather different techniques, a unified description from -20 to $+20$ eV has been drawn from many sources.[17,22–33] The Fermi level E_F lies 4.4 eV below the vacuum.[17] With respect to E_F, the conduction-band (CB) edge E_C is at 0.75 eV and the valence-band (VB) edge E_V, at -0.95 eV.

The VB shows two main structures approximately Gaussian in shape; the first peak due to $3p$ electrons is centered around -3 eV with a width of about 3 eV.[25,26,28] The second peak at -7.5 eV is wider ($\sim$8 eV); considering this peak as originating from $3s$ electrons,[25] both peaks present an integral of two states per atom, i.e., 8.6×10^{22} cm^{-3}. In hydrogenated material, states appear around -6.3 and -11 eV due to SiH, Si_2H, and Si_3H bonds[25] but their overall effect is weak and they are not considered here. The CB has little structure and presents a constant EDOS above 2.22 eV.[28,33] Both bands are considered parabolic near their edges.[27,30] The localized states are described by exponential tails of characteristic energies kT_c of 50 and 27 meV for the valence- and conduction-band tails, respectively[31,32] plus a Gaussian distribution of deep states at -0.25 eV.[23]

These various structures are normalized and adjusted to provide a continuous EDOS. The result is presented in Fig. 1 with the details of the localized states shown in Fig. 2. In the following expressions, E is in eV and $g(E)$ in eV^{-1} cm^{-3}:

$$g(E)=10^{22}\exp\left[-\frac{(E+7.5)^2}{23.53}\right]+2.68\times10^{22}\exp\left[-\frac{(E+2.9)^2}{3.28}\right], \quad E\leqslant-2.0 \quad (14)$$

$$2.28\times10^{22}\sqrt{-E-0.92}, \quad -2.0<E<-0.95$$

$$4\times10^{21}\exp\left[\frac{-E-0.95}{0.050}\right]+10^{16}\exp\left[-\frac{(E+0.25)^2}{0.045}\right]+4\times10^{21}\exp\left[\frac{E-0.75}{0.027}\right], \quad -0.95\leqslant E\leqslant0.75$$

$$2.28\times10^{22}\sqrt{E-0.72}, \quad 0.75<E<2.22$$

$$2.79\times10^{22}, \quad E\geqslant2.22.$$

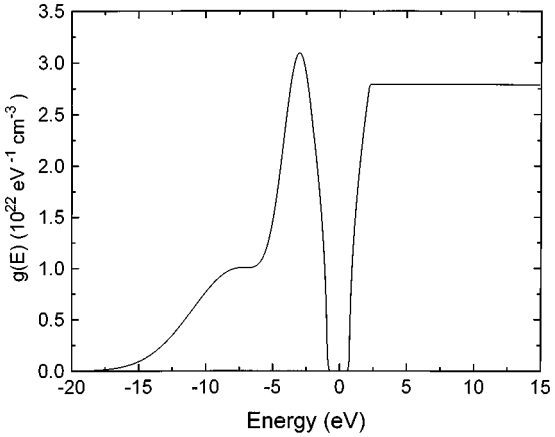

FIG. 1. Density of electronic states, showing the main features of the valence and conduction bands.

C. Ionization rates

We first write, for an electron of incident energy E, the rate of ionization of an electron in the valence band, leaving two resulting electrons at energies E_1 and E_2 in the conduction band and a hole at energy ε in the valence band. From Fermi's golden rule,

$$n(E,E_1,E_2,\varepsilon)dE_1\,dE_2\,d\varepsilon$$

$$=A_{ie}g(E_1)[1-f(E_1)]g(E_2)[1-f(E_2)]g(\varepsilon)f(\varepsilon)\times\delta(E-E_1-E_2-|\varepsilon|)dE_1\,dE_2\,d\varepsilon, \tag{15}$$

where the matrix element A_{ie} is supposed to be energy independent.[16] Due to energy conservation, the final state is uniquely defined by the energies of two of the final carriers, say E_1 and E_2. Moreover, the rate is zero for both E_2 and ε lying into the mobility gap since we excluded transitions between two localized states (cf. Sec. III A). Integrating over allowed values of E_2 and ε, the rate of ionization by an electron of energy E, leaving one of the resulting electrons between E_1 and E_1+dE_1, is obtained:

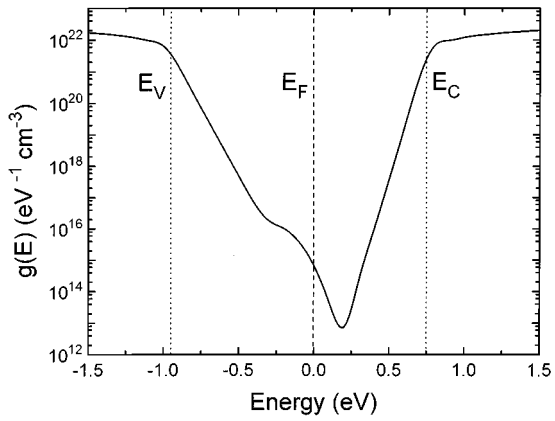

FIG. 2. Details of the density of states between E_V and E_C. In the text, E_F is taken as the origin.

$$n(E,E_1)dE_1=A_{ie}g(E_1)[1-f(E_1)]dE_1\times\int_{\mathrm{VB}}d\varepsilon\; g(\varepsilon)f(\varepsilon)g(E-E_1-|\varepsilon|)\times[1-f(E-E_1-|\varepsilon|)]. \tag{16}$$

A similar expression is found for $p(\varepsilon,\varepsilon_1)d\varepsilon_1$ due to holes of energy ε. Plots of $n(E,E_1)dE_1$ and $p(\varepsilon,\varepsilon_1)d\varepsilon_1$, calculated with the a-Si:H EDOS presented in the previous section, are shown in Fig. 3 for different initial energies of electrons and holes. Note that the integral of the final carrier distribution increases with the incident energy since the total number of available final states increases. New integrations over E_1 or ε_1 yield the total ionization rates $W_{ie}(E)$ and $W_{ih}(\varepsilon)$:

$$W_{ie}(E)=A_{ie}\int_{E_F}^{E}dE_1\; g(E_1)[1-f(E_1)]\int_{-E}^{E_F}d\varepsilon\times g(\varepsilon)f(\varepsilon)g(E-E_1-|\varepsilon|)[1-f(E-E_1-|\varepsilon|)], \tag{17}$$

$$W_{ih}(\varepsilon)=A_{ih}\int_{\varepsilon}^{E_F}d\varepsilon_1\; g(\varepsilon_1)f(\varepsilon_1)\int_{E_F}^{|\varepsilon|}dE\; g(E)\times[1-f(E)]g(\varepsilon+E-\varepsilon_1)f(\varepsilon+E-\varepsilon_1), \tag{18}$$

where the integrations are performed over all energetically available states, both localized and extended, of the respective bands with the above-mentioned constraint.

1. Ionization rates in c-Si

Let us first calculate $W_{ie}(E)$ for the simple case of pure parabolic bands with a gap of 1.1 eV as an approximation of c-Si. Figure 4 presents our calculation and the parametric equation (7) used by Drummond and Moll,[16] compared with Kane's more exact calculation.[12] All curves have been normalized to the same reference energy of 5.56 eV, i.e., 5 eV above E_C. The rate derived from parabolic bands is in excellent agreement with Kane's result below 2 eV and above 5 eV. However, $W_i(E)$ is overestimated by a factor of 1.5 to 2 between 2.5 and 4 eV. The parametric equation (7) gives excellent results in the range of 2.5–6 eV but underestimates the ionization rate by a factor of 5 below 2 eV and overestimates it by 30% above 6 eV.

2. Ionization rates in a-Si:H

The electron ionization rate $W_{ie}(E)$ in a-Si:H is calculated with Eq. (17) using our realistic EDOS [Eq. (14)]. The result is shown in Fig. 4, compared with results in c-Si, all normalized at 5.56 eV above E_F. Our curve in a-Si:H and Kane's results in c-Si are identical above 4 eV where the ionization rate becomes less sensitive to the EDOS, c-Si and a-Si:H then appearing as similar materials far from the band edge; at lower energy, the ionization rate is significantly less in a-Si:H due to its wider band gap. We thus take W_{ie} and the ionization mean free path λ_{ie} in a-Si:H as equal to the

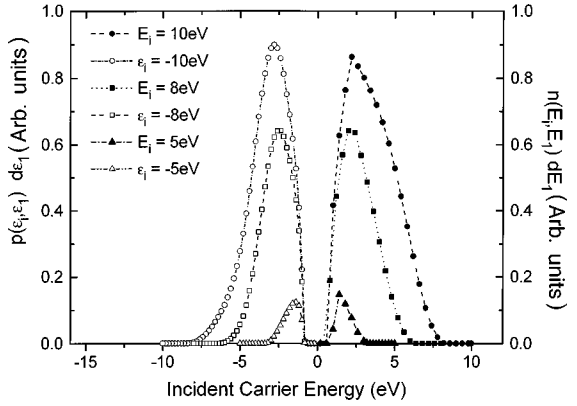

FIG. 3. Curves of $n(E,E_1)dE_1$ and $p(\varepsilon,\varepsilon_1)d\varepsilon_1$ in a-Si:H for various values of the initial energies E and ε.

c-Si values at the calibration point, i.e., 5 eV above E_C. Similar results are found for holes.

D. Phonon emission rates in a-Si:H

Since the electron-phonon coupling in a crystalline material is maximum for high-frequency phonons, all previous studies of ε_p in crystals have only considered the emission of Raman phonons of energy $\hbar\omega_r$ as the nonionizing energy-loss mechanism for hot carriers. In c-Si, $\hbar\omega_r=63$ meV.

The vibrational densities of states (VDOS's) of c-Si and a-Si:H have been compared by Kamitakahara *et al.*[35] While the VDOS in a-Si:H understandably does not present the well-defined discontinuities associated with critical points, it nevertheless shows a clear resemblance to its crystalline counterpart. In particular, a broad peak in a-Si:H centered at 60 meV corresponds to the narrow peak at 60 meV due to TO phonons in c-Si. We then conclude that phonon scattering of hot carriers in a-Si:H can be realistically described by the emission of high-energy phonons of 60 meV only. Assuming an energy-independent coupling, as in c-Si, Fermi's golden rule yields scattering rates that only depend on the available EDOS of states at the carrier's final energy,

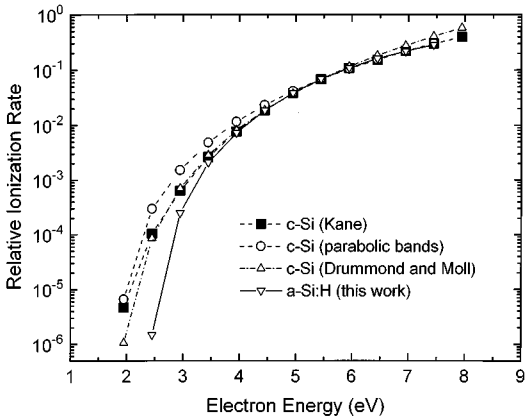

FIG. 4. Calculated ionization rates for electrons in c-Si and a-Si:H. The c-Si data for pure parabolic bands are presented together with Drummond and Moll's empirical equation (Ref. 16) and Kane's results (Ref. 12). All curves are normalized at 5.56 eV.

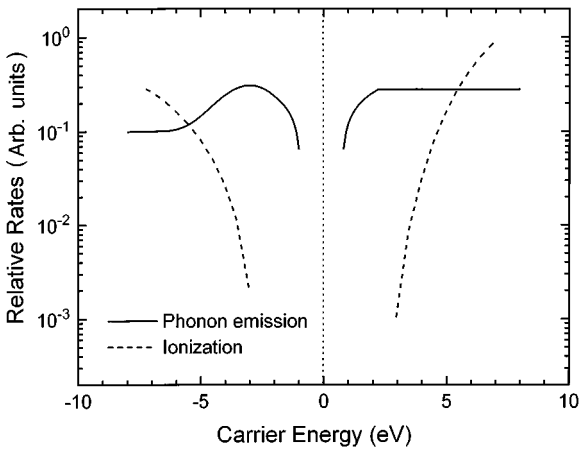

FIG. 5. Ionization and phonon emission rates for holes (negative energies) and electrons (positive energies) in a-Si:H. The relative normalizations between the phonon and ionization rates are arbitrarily set to $r=1$ at 5.56 eV from E_F for both electrons and holes. The normalization between the electron- and hole-scattering rates is arbitrary.

$$W_{re}(E)=A_{re}g(E-\hbar\omega_r)[1-f(E-\hbar\omega_r)], \tag{19}$$

$$W_{rh}(\varepsilon)=A_{rh}g(\varepsilon+\hbar\omega_r)f(\varepsilon+\hbar\omega_r), \tag{20}$$

with A_{re} and A_{rh} constant. Figure 5 shows the energy dependence of W_{re} and W_{rh} in a-Si:H.

Phonon emission mean free paths in a-Si:H

The mean free path λ_r for the emission of a phonon of energy $\hbar\omega_r$ is simply the mean distance a carrier must travel to transfer the energy $\hbar\omega_r$ to the network through electron-phonon interactions. Since no measured value of λ_r in a-Si:H was available, we attempted a measurement of photocurrent multiplication in p-i-n diodes optimized to withstand high reverse biases.[11,35] The p-i or n-i interface was illuminated with 632 nm light from a HeNe laser with an absorption length of 0.5–1 μm, which is short enough compared to the 3–15-μm i layer but long enough to reach through the 30- and 500-nm doped layers. The beam was mechanically strobed at 250 Hz and the signal was fed into a lock-in amplifier to extract the photocurrent from the leakage current. The setup was tested with a c-Si avalanche photodiode (RCA C30817) and multiplication was observed above 100 V. Figure 6 shows the photocurrents observed in a 4-μm a-Si:H diode. The increase in the photocurrent below 50 V is due to the buildup or the depletion layer from the p-i to the n-i interface. No multiplication is observed in this sample up to electric fields of 5.5×10^5 V/cm. The highest field that could be reached was 6.9×10^5 V/cm on a 5.6-μm diode. Still, no multiplication could be seen above the leakage current fluctuations of 10% near the breakdown voltage. This results in a multiplication coefficient lower limit of $M(F)<1.1$ at 6.9×10^5 V/cm.

When Baraff's theory of secondary ionization[36] is used to extract λ_r from the field dependence of $M(F)$ in c-Si, values from 50 to 70 Å are reported depending upon whether ionization threshold energies, $E_i=E_g$ or $E_i=\frac{3}{2}E_g$ are used.[37] Using the same procedure, our measurement leads to upper

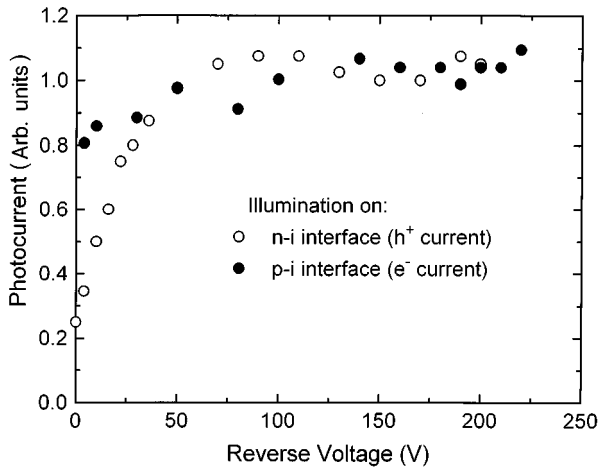

FIG. 6. Measured photocurrents for electrons and holes.

limits of 17 or 22 Å in *a*-Si:H. In both cases, the upper limit in *a*-Si:H is a factor of 3 less than λ_r in *c*-Si. We note that our upper limit is similar to the value of 10–20 Å measured[38,39] in another amorphous semiconductor, *a*-Se, for which multiplication has been observed at fields of 10^6 V/cm, just above the highest field reached in *a*-Si:H.

E. Relative normalization of ionization and phonon emission rates

For our simulation, only the ratios A_{re}/A_{ie} and A_{rh}/A_{ih} are needed in order to normalize the ionization and phonon emission rates shown in Fig. 5. For electrons, we define the parameter r as the value of the ratio between the interaction rates at $E=5.56$ eV, which is the same normalization energy used by Drummond and Moll:[16]

$$r=r_e(E=5.56\ \text{eV})=\frac{W_{re}(5.56\ \text{eV})}{W_{ie}(5.56\ \text{eV})}=\frac{\lambda_{ie}(5.56\ \text{eV})}{\lambda_{re}(5.56\ \text{eV})}, \tag{21}$$

from which the ratio A_{re}/A_{ie} may be determined. Since no normalization value is known for holes, we use the same ratio between the proportionality constants as for electrons, i.e., $A_{rh}/A_{ih}=A_{re}/A_{ie}$. To ensure that this particular choice does not significantly affect the result of the simulation, tests with different values of A_{rh}/A_{ih} will serve to measure the sensitivity of ε_p on this parameter.

As mentioned in Secs. III C and III D, it is assumed that $\lambda_i(5.56\ \text{eV})$ is identical in *c*-Si and *a*-Si:H and that $\lambda_{r_{a\text{-Si:H}}} < \frac{1}{3}\lambda_{r_{c\text{-Si}}}$ near the band edge. For the purpose of the calculation, the upper limit of $\frac{1}{3}\lambda_{r_{c\text{-Si}}}$ is used and the hypothesis is made that this factor of $\frac{1}{3}$ measured near the band edge holds at 5.56 eV such that $r_{a\text{-Si:H}} \gtrsim 3r_{c\text{-Si}}$.

Despite the value $r_{c\text{-Si}}=3.2$ measured by Bartelink *et al.*[17] and due to different simplifying hypotheses in their models, Drummond and Moll had to use $r_{c\text{-Si}}=0.6$ to find $\varepsilon_p=3.6$ eV.[16] Instead of deriving our value of $r_{a\text{-Si:H}}$ from an arbitrarily chosen value of $r_{c\text{-Si}}$, we first use our Monte Carlo in *c*-Si to find the value of $r_{c\text{-Si}}$ that will yield $\varepsilon_{p_{c\text{-Si}}}=3.63$ eV. We then take 3 times this $r_{c\text{-Si}}$ as our ''standard'' value of $r_{a\text{-Si:H}}$; this is actually a lower limit and simulations will be made with different values of $r_{a\text{-Si:H}}$ around this ''standard'' one (cf. Sec. IV).

F. Monte Carlo algorithm

Before running the Monte Carlo simulation, the interaction rates are calculated for the material's DOS from Eqs. (17)–(20). The ionization and phonon emission rates for each type of carrier are then normalized with some input value of the parameter r discussed in the last section. The ionization probabilities $P_{0(e,h)}(E)$ are then evaluated (Eq. (5)) for energies in the range -15 to $+19$ eV, relative to E_F, in steps of $\Delta E=0.01$ eV for $|E|<3$ eV where the rates change more rapidly, $\Delta E=0.05$ eV for 3 eV$<|E|<5$ eV and $\Delta E=1$ eV for $|E|>5$ eV. It has been checked that using small steps $\Delta E=0.01$ eV over the whole energy range would not improve the accuracy. During the simulation, the same energy range is discretized in equal $\Delta E=0.01$ eV intervals and the electron and hole distributions are stored in two long vectors, the elements of which record the number of electrons or holes in the interval ΔE. The carrier energy is then reduced by six energy steps at each phonon emission event. Before the simulation, these vectors are loaded with some initial populations:

$$N_e(E_i)=N_eS_e(E_i)\Delta E, \quad i=1,n$$

$$N_h(\varepsilon_j)=N_hS_h(\varepsilon_j)\Delta\varepsilon, \quad j=1,p, \tag{22}$$

where i (j) is the electron (hole) vector element index, n (p) is the number of electron (hole) elements in the vector, N_e and N_h are the total number of injected carriers of each type, and $S_e(E)$ and $S_h(\varepsilon)$ are their normalized energy distributions. In a typical simulation, the initial number of carriers is about 100. The total injected energy is

$$E_{\text{tot}}=\sum_{i=1}^{n} E_iN_e(E_i)+\sum_{j=1}^{p}\varepsilon_jN_h(\varepsilon_j). \tag{23}$$

From this starting point, the simulation proceeds according to the following algorithm. We first start with the electron in the highest occupied energy bin and calculate its ionization probability from a Lagrange interpolation of order 5 on the previously calculated values of $P_{0e}(E)$. A random number R, uniformly distributed between 0 and 1, is then drawn to select the next interaction event, which is ionization if $R<P_{0e}(E)$ and phonon emission otherwise. In a phonon event, $N_e(E)$ is reduced by 1 while $N_e(E-\hbar\omega_r)$ is incremented and the amount $\hbar\omega_r$ is added to E_{re}, the total phonon energy loss for electrons. For an ionization event, the final state, made of one hole at ε and two electrons at E_1 and E_2, is randomly selected according to a probability that is proportional to Eq. (15). The calculation of Eq. (15) for all allowed final states that are determined by E_1 and E_2 and the random selection of E_1 and E_2 is the most time consuming part of the simulation. $N_e(E)$ is then decremented while $N_e(E_1)$, $N_e(E_2)$, and $N_h(\varepsilon)$ are incremented; one electron-hole pair has thus been added to the cascade.

The next carrier to be considered is again the highest-lying electron; all electrons are thus processed until no more

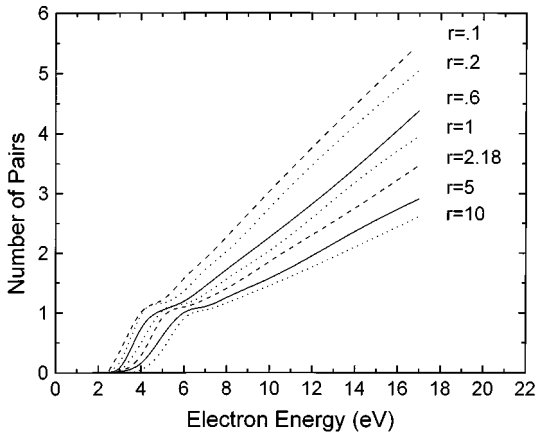

FIG. 7. Number of pairs produced by hot electrons in c-Si calculated from interaction rates given by Drummond and Moll (Ref. 16) for various values of the normalization r.

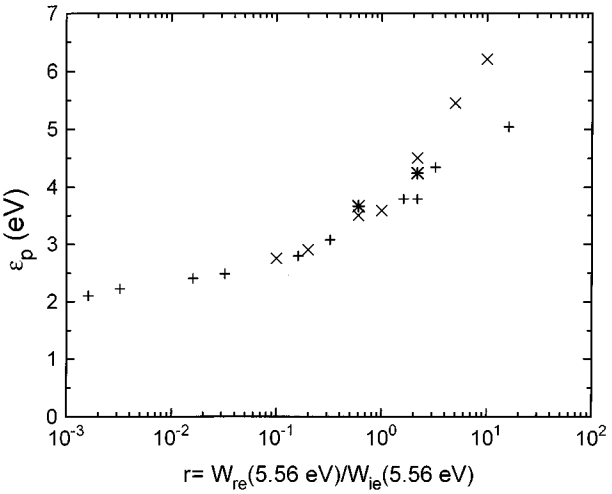

FIG. 8. Values of ε_p in c-Si as a function of r. (*) are results given by Drummond and Moll (Ref. 16), ($\times$) are results from this work using the same interaction rates as Ref. 16, and (+) are results obtained from a parabolic band model.

electrons are found above $E_C+\hbar\omega_r$. The same procedure is then applied to holes until all holes below $E_V-\hbar\omega_r$ are consumed. We then go back to electrons that may have been produced by holes and so forth until all carriers are within $\hbar\omega_r$ of the mobility gap. Since ionization between two localized states is excluded, the cascade is then over and the simulation is stopped. The final distributions and the values of E_{re} and E_{rh} are then available. It is easily verified that N_e and N_h have been increased by the same amount n_p and that the energy has been conserved, i.e.,

$$E_{\text{tot}}=\sum_{i=1}^{n} E_i N_e(E_i)+\sum_{j=1}^{p} \varepsilon_j N_h(\varepsilon_j)+E_{re}+E_{rh}. \quad (24)$$

IV. RESULTS

A. c-Si

Simulations have been made in c-Si for three main reasons: (1) to test our algorithm with the simple model used by Drummond and Moll in an attempt to reproduce their results, (2) to improve results in c-Si by using somewhat more realistic interaction rates, and (3) to find a realistic value of r that would yield $\varepsilon_p=3.63$ eV in c-Si from which our ''standard'' value of $r_{a\text{-Si:H}}$ will be determined.

The first simulation is made with the interaction rates used by Drummond and Moll. $W_i(E)$ is given by Eq. (7), which is in good agreement with Kane's calculations, and W_r is taken as constant; interaction rates are the same for electrons and holes. Figure 7 shows curves of $n_p(E)$, the number of pairs produced by electrons of initial energy E, for values of r from 0.1 to 10. Curves for holes are identical. Above a few eV, $n_p(E)$ increases linearly with E such that ε_p becomes independent of E as expected. Figure 8 shows ε_p as a function of r from these simulations ($\times$). Drummond and Moll's values for $r=0.6$ and $r=2.18$ are also shown (*). It is indeed observed that, within the Monte Carlo statistical fluctuations, Drummond and Moll's results are reproduced by our simulations. But the low value $r=0.6$ that must be used to reproduce ε_p shows that the assumption of constant phonon scattering rates is not realistic.

Simulations are now made for pure parabolic bands. Here again, $W_{i(e,h)}(E)$ is well described by Eq. (7) but $W_{r(e,h)}(E)$ is proportional to $\sqrt{|E|-0.56\ \text{eV}-\hbar\omega_r}$ and decreases near the band edges. As a consequence, the energy loss to phonons and, therefore, ε_p are expected to decrease for a given value of r. Indeed, results presented in Fig. 8 (+) indicate that ε_p is now significantly lower for $r>1$. At $r=2.18$, $\varepsilon_p=4$ eV in better agreement with the experimental result than previously found. $\varepsilon_p=3.63$ eV is now obtained with $r=1.35$, a more acceptable value than $r=0.6$. These results demonstrate the procedure's validity and we now proceed with simulations in a-Si:H.

B. a-Si:H

The interaction rates used in a-Si:H were calculated with Eqs. (17)–(20) with the DOS given by Eq. (14). Simulations

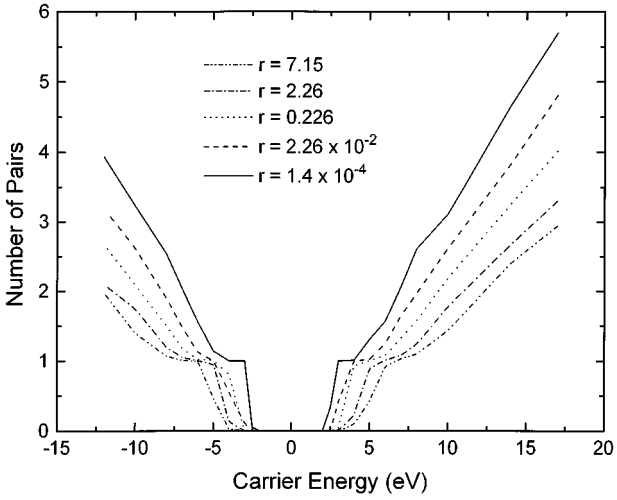

FIG. 9. Number of pairs produced by hot carriers in a-Si:H for various values of the normalization r.

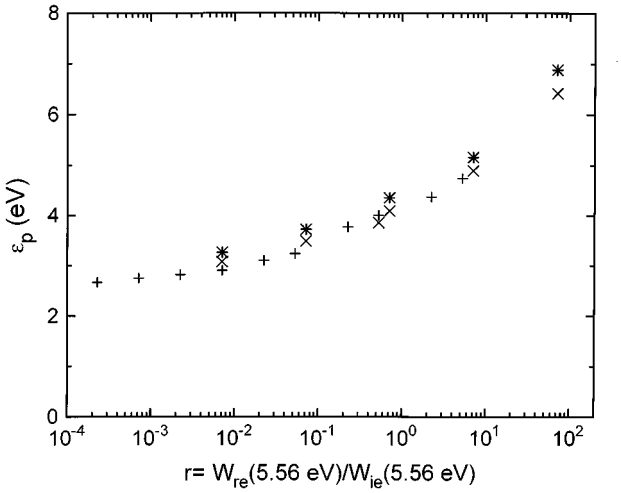

FIG. 10. Values of ε_p in a-Si:H as a function of r due to monoenergetic initial electrons (+), initial energy distributions produced by photons (×) and with a fivefold increase of the phonon generation rate by holes $A_{rh}/A_{ih}=5A_{re}/A_{ie}$ (∗).

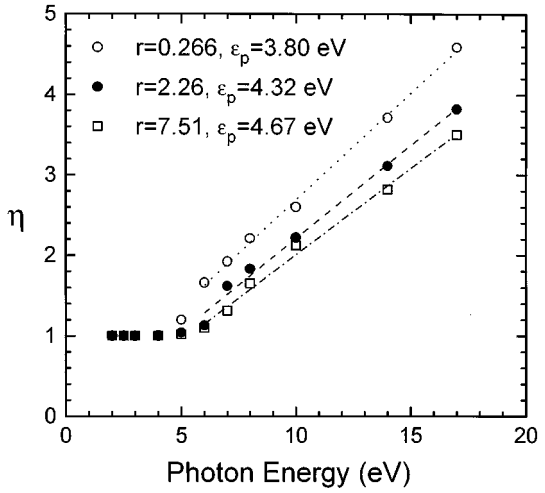

FIG. 12. Quantum efficiency in a-Si:H as a function of the photon's energy for three values of r.

are first generated starting with monoenergetic carrier distributions for several values of r. Curves of $n_p(E)$ are shown in Fig. 9; curves for electrons and holes look very similar. Although no ionization threshold energy was imposed, some effective threshold is clearly observed at about 2.5 eV, i.e., about $1.5E_g$. Above 5 eV, $n_p(E)$ is almost linear with variations from linearity that could be statistical. Figure 10 shows values of ε_p for monoenergetic electrons as a function of r (+); values for holes are almost identical. Our ''standard'' value $r_{a\text{-Si:H}}=3r_{c\text{-Si}}=4$ yields $\varepsilon_p=4.6$ eV, somewhat higher than our experimental value of about 4 eV.[9–12] $r=3$ would give $\varepsilon_p\sim4.4$ eV, the upper experimental limit.

In addition to simulations of monoenergetic carriers, initial carrier distributions produced by the absorption of UV photons have been calculated according to Eq. (11) to evaluate the optical quantum efficiency $\eta(E_\gamma)$ in a-Si:H. Figure 11 shows initial carrier distributions for 5- and 10-eV photons and Fig. 12 presents curves of $\eta(E_\gamma)$ for three values of r. Values of ε_p obtained from these curves (× in Fig. 10) are almost identical to those previously found, indicating that ε_p is quite insensitive to the details of the initial distributions. Other simulations made with ratios A_r/A_i that were five times larger for holes than for electrons (∗ in Fig. 10) indicate that shorter mean free paths for holes would cause ε_p to increase only slightly.

An important goal of the simulations was to assess the effect of the intragap states of amorphous semiconductors on the value of ε_p. Compared with crystalline semiconductors, ionization is now possible for carriers below the ionization threshold of a crystalline semiconductor with the same gap since transitions are now allowed toward final states in which, out of the three carriers, one or two have been created in the gap. This would increase the number of ionization

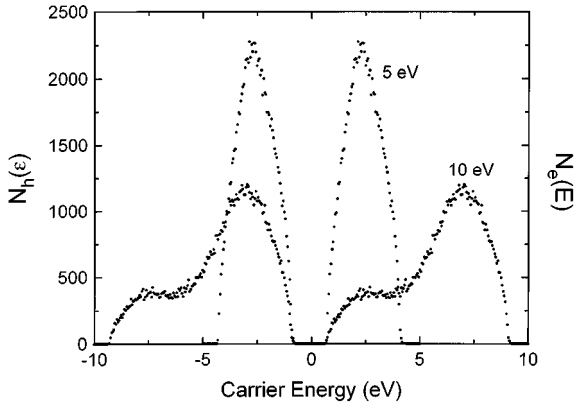

FIG. 11. Initial energy distributions of hot carriers produced in a-Si:H by the absorption of photons of 5 and 10 eV as calculated from Eq. (11).

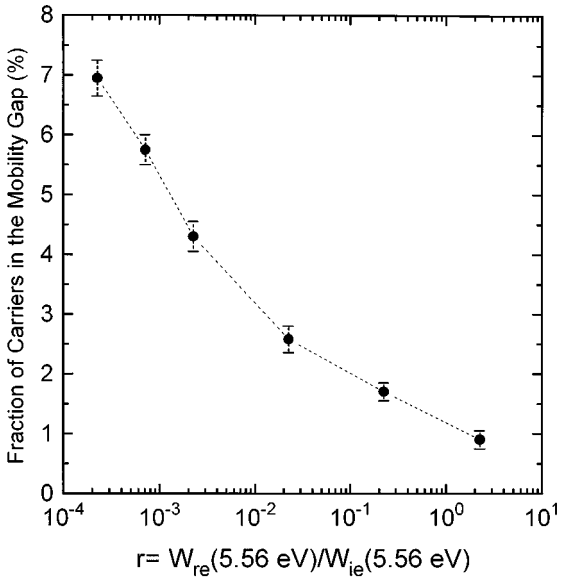

FIG. 13. Fraction of carriers that are produced directly in the localized states by an ionization event.

events but some of the carriers could remain in the localized states[40] and not contribute to the signal. Some of these carriers could nevertheless take part in the signal through thermal reemission or field-assisted detrapping. The effective ε_p could then increase with the applied electric field, possibly following Onsager's theory of geminate recombination[41] as was suggested by our measurements[9,42] and measurements of photogeneration in a-Si:H by Carasco and Spear.[43] Figure 13 shows the fraction of the carriers in the gap states at the end of a cascade produced by 10-eV photons as a function of r. For reasonable values of r, less than 1% of the final populations are in the gap and r should be lowered by many orders of magnitude before this fraction becomes significant. Clearly, these simulations indicate that the intragap states play a negligible role in the cascade process. Although some carriers are created in the gap, the process is infrequent because W_i, though nonzero, decreases steeply near the band edge and W_r is soon completely dominant. The density of states in the gap could be increased by orders of magnitude before this process would play any significant role.

V. DISCUSSION

This Monte Carlo has been developed to perform a detailed simulation of hot carrier thermalization in c-Si and a-Si:H in order to understand the surprisingly low value of ε_p in the range 3.4–4.4 eV measured in a-Si:H. Although the actual simulations may require long calculations, the model is conceptually simple and could be applied to any semiconductor or insulator by introducing the proper EDOS. From a given EDOS, the energy dependence of ionization and phonon emission rates, W_i and W_r, are calculated in the random-**k** approximation, which has been shown to be justified by Kane.[12] The model also requires that the relative value of $r=W_r/W_i$ be known at some energy to normalize these rates.

One of the main results of the simulations, which is valid in c-Si and a-Si:H, is that ε_p is independent of the carrier's initial energy as long as this energy is a few eV above the band edge, a fact that was also observed by Drummond and Moll.[16] This clearly shows that ε_p is determined by thermalization processes at the very end of the cascade, in agreement with the well-known experimental fact that ε_p is independent of the energy from a few eV up to many GeV. Another important result is that ε_p varies slowly with r (Figs. 8 and 10); in the region of interest, the dependence is approximately logarithmic instead of linear. It is also observed that ε_p is somewhat sensitive to the details of the EDOS and not only to E_g. These last two observations contradict the main hypotheses of models based on simple arguments of energy balance developed by Shockley,[5] Klein,[6] and others.

Simulations performed in c-Si provide results which are identical to those of Drummond and Moll[16] when the same interaction rates are used (Fig. 8) although our calculation spans a much broader range of the parameter r. With rates derived from parabolic bands and that allow W_r to decrease near the band edge, $\varepsilon_p=3.63$ eV is found in c-Si with a normalization $r=1.35$ in better agreement with photoemission data than $r=0.6$, necessary with the rates used by Drummond and Moll. The discrepancy with the actual value $r=2.18$ could be due to some simplification of the model as the use of pure parabolic bands, the constant matrix elements A_i and A_r or the random-**k** approach.

The same algorithm is then used in a-Si:H using the EDOS from Eq. (14). A value of r somewhat more than three times larger than in c-Si is used to account for the absence of multiplication in our a-Si:H p-i-n diodes under high reverse bias. A value $r_{a\text{-Si:H}}\approx 4$ would then lead to $\varepsilon_p\approx 4.6$ eV in reasonable agreement with our measurements. From Fig. 10, our experimental range would translate into a range of r from 0.1 to 4. Values $r<3$ are excluded from our photocurrent measurements. Values of ε_p above 4.4 eV must be rejected since this is an absolute limit corresponding to the highest amount of collected charge actually measured in our detectors. A result $r\approx 3$, yielding $\varepsilon_p\approx 4.4$ eV would then seem reasonable while values of $\varepsilon_p\approx 5.8$ eV predicted by Klein's model and of $\varepsilon_p=6$ eV measured by Kaplan *et al.*[44] are excluded. While it could be argued that our measurements in a-Si:H detectors at high field underestimate ε_p due to signal multiplication, this is refuted by the fact that no multiplication could be observed during dedicated photocurrent measurements. It then seems more probable that insufficient collection efficiency would have led to overestimated values of ε_p in Ref. 44, the agreement with Klein's model being fortuitous.

The small difference between ε_p in c-Si and a-Si:H, despite much larger values of E_g and r in a-Si:H, and the discrepancy with Klein's model[6] is explained by the fact that ε_p is found to increase slowly with r, almost logarithmically, instead of linearly as assumed in Klein's and other simple models.[5,6] Also, since the avalanche probability at high field decreases exponentially with r,[36] materials in which little or no multiplication is observed can still exhibit reasonably low values of ε_p.

From the energy distribution of carriers at the end of the thermalization process, it is found that very few carriers are produced in the localized states by ionization events, indicating that possible extraction of these carriers by the external field before geminate recombination could not lead to a field-dependent value of ε_p. This contradicts one of our earlier hypotheses[9,43] proposed to explain the observed field-dependent collection efficiency. Two other possible effects, namely, fast recombination of carriers from neighboring pairs and monomolecular recombination, are still possible in the very high carrier density track produced by an ionizing particle.[11,42]

VI. CONCLUSION

The model presented here answered many of our interrogations concerning the process of pair creation by energetic particles in a-Si:H and c-Si. Monte Carlo simulations in c-Si, using interaction rates derived from parabolic bands that allow W_r to decrease near the band edge, provided improvement over similar calculations made by Drummond and Moll.[16] Similar simulations in a-Si:H have reproduced our experimental value of ε_p and explained why ε_p in a-Si:H is lower than was first expected from simple models. From the simulated final carrier distributions, the Onsager effect is not expected to contribute to the observed field-dependent charge collection efficiency in a-Si:H.

This work constitutes a detailed analysis of pair creation by energetic ionizing particles in an amorphous semiconductor. But despite the results achieved, some questions remain unanswered. First, uncertainties over the value of r in a-Si:H should be resolved. Also, the discrepancy between $r=1.35$ which must be used in c-Si and the actual value of $r=2.18$ is taken as an indication that the model could be improved. In particular, the energy dependence of A_i and A_r should be considered.

ACKNOWLEDGMENTS

We wish to thank R. Bornais and B. Lorazo from the Groupe de physique des particules for their assistance in providing computing facilities and A. Yelon for his comments on the manuscript. This work is supported by the Natural Sciences and Engineering Research Council of Canada (NSERC) and the Fonds Québécois pour la Formation des Chercheurs et l'Aide à la Recherche (FCAR).

*Present address: Department of Physics, Carleton University, Ottawa, Canada K1S 5B6. Electronic address: Dubeau@Physics.Carleton.CA

†Electronic address: Hamel@LPS.UMontreal.CA

‡Present address: Centre d'Études Nucléaires, Saclay, France; Electronic address: Pochet@Serin.CEA.FR

[1] F. E. Emery and T. A. Rabson, Phys. Rev. **140**, A2089 (1965).

[2] C. A. Klein, J. Phys. Soc. Jpn. **21**, 307 (1966).

[3] A. Rothwarf, J. Appl. Phys. **44**, 752 (1973).

[4] K. G. McKay, Phys. Rev. **84**, 829 (1951).

[5] W. Shockley, Solid-State Electron. **2**, 35 (1961).

[6] C. A. Klein, J. Appl. Phys. **39**, 2029 (1968).

[7] R. C. Alig, S. Bloom, and C. W. Struck, Phys. Rev. B **22**, 5565 (1980).

[8] T. Pochet, J. Dubeau, L. A. Hamel, B. Equer, and A. Karar, in *Amorphous Silicon Technology—1989*, edited by A. Madan, M. J. Thompson, P. C. Taylor, Y. Hamakawa, and P. G. LeComber, MRS Symposia Proceedings No. 149 (Materials Research Society, Pittsburgh, 1989), p. 661.

[9] L. A. Hamel, J. Dubeau, T. Pochet, and B. Equer, IEEE Trans. Nucl. Sci. **38**, 251 (1991).

[10] J. Dubeau, T. Pochet, L. A. Hamel, B. Equer, and A. Karar, Nucl. Instrum. Methods Phys. Res. Sect. B **54**, 458 (1991).

[11] J. Dubeau, Ph.D. thesis, Université de Montréal (1992).

[12] E. O. Kane, Phys. Rev. **159**, 624 (1967).

[13] C. N. Berglund and W. E. Spicer, Phys. Rev. **136**, A1030 (1964).

[14] D. Long, Phys. Rev. **120**, 2024 (1960).

[15] C. Y. Duh and J. L. Moll, Solid-State Electron. **11**, 917 (1968).

[16] W. E. Drummond and J. L. Moll, J. Appl. Phys. **42**, 5556 (1971).

[17] D. L. Bartelink, J. L. Moll, and N. I. Meyer, Phys. Rev. **130**, 972 (1963).

[18] E. Antončik, G. Di Cola, and L. Farese, Radiat. Eff. **5**, 1 (1970).

[19] J. Tauč, J. Phys. Chem. Solids **8**, 219 (1959).

[20] L. R. Canfield, J. Kerner, and R. Korde, Appl. Opt. **28**, 3940 (1989).

[21] T. Tiedje and A. Rose, Solid State Commun. **37**, 49 (1980).

[22] G. Müller, H. Mannsperger, and S. Kalbitzer, Philos. Mag. B **53**, 257 (1986).

[23] I. Sakata and Y. Hayashi, Appl. Phys. A **37**, 153 (1985).

[24] J. Kocka, M. Vanecek, and A. Triska, in *Amorphous Silicon and Related Materials*, edited by H. Fritzsche (World Scientific, New York, 1988), p. 297.

[25] L. Ley, in *The Physics of Hydrogenated Amorphous Silicon II*, edited by J. D. Joannopoulos and G. Lucovski, Electronic and Vibrational Properties Vol. 61 (Springer-Verlag, New York, 1964).

[26] R. Karcher, L. Ley, and R. L. Johnson, Phys. Rev. B **30**, 1896 (1984).

[27] W. B. Jackson, S. J. Oh, C. C. Tsai, and J. W. Allen, Phys. Rev. Lett. **53**, 1481 (1984).

[28] W. B. Jackson, S. M. Kelso, C. C. Tsai, J. W. Allen, and S. J. Oh, Phys. Rev. B **31**, 5187 (1985).

[29] S. Griep and L. Ley, J. Non-Cryst. Solids **59-60**, 253 (1983).

[30] J. Tauč, in *Amorphous and Liquid Semiconductors*, edited by J. Tauč (Plenum, London, 1974), Chap. 4.

[31] T. Tiedje, in *Hydrogenated Amorphous Silicon*, edited by J. Pankove, Semiconductors and Semimetals Vol. 21C (Academic, New York, 1984), p. 207.

[32] R. A. Street and D. K. Biegelsen, in *The Physics of Hydrogenated Amorphous Silicon II*, edited by J. D. Joannopoulos and G. Lucovski, Electronic and Vibrational Properties Vol. 61 (Springer-Verlag, New York, 1964).

[33] J. Reichardt, L. Ley, and R. L. Johnson, J. Non-Cryst. Solids **59-60**, 329 (1983).

[34] W. A. Kamitakahara, C. M. Soukoulis, H. R. Shanks, U. Buchenau, and G. S. Grest, Phys. Rev. B **36**, 6539 (1987).

[35] T. Pochet, J. Dubeau, B. Equer, A. Karar, and L. A. Hamel, J. Appl. Phys. **68**, 1340 (1990).

[36] G. A. Baraff, Phys. Rev. **128**, 2507 (1962).

[37] C. A. Lee, R. A. Logan, R. T. Batdorf, J. J. Kleinmack, and W. Wiegman, Phys. Rev. **134**, A761 (1964).

[38] Y. Takasaki, K. Tsuji, T. Hirai, E. Maruyama, K. Tanioka, J. Yamazaki, K. Shidara, and K. Taketoshi, in *Amorphous Silicon Technology*, edited by A. Madan, M. J. Thompson, P. C. Taylor, P. G. LeComber, and Y. Hamakawa, MRS Symposia Proceeding No. 118 (Materials Research Society, Pittsburgh, 1988), p. 387.

[39] K. Tsuji, Y. Takasaki, T. Hirai, and K. Taketoshi, J. Non-Cryst. Solids **114**, 94 (1989).

[40] C. C. Eugster and P. L. Hagelstein, IEEE J. Quantum. Electron. **26**, 75 (1990).

[41] L. Onsager, Phys. Rev. **54**, 554 (1938).

[42] T. Pochet, Ph.D. thesis, Université de Montréal (1991).

[43] F. Carasco and W. E. Spear, Philos. Mag. B **47**, 495 (1983).

[44] S. N. Kaplan, I. Fujieda, V. Perez-Mendez, S. Qureshi, W. Ward, and R. A. Street, Nucl. Instrum. Methods Phys. Res. Sect. A **273**, 611 (1988).